Wave Response Analysis for Pontoon-type Pier:
Very Large Floating Structure

Sang-Do Lee[*] · Sung-Hyeon Park[**†] · Gil-Young Kong[***]

* Graduate School of Korea Maritime and Ocean University, Busan 49112, Korea

** Mokpo National Maritime University, Mokpo 58628, Korea

*** Korea Maritime and Ocean University, Busan 49112, Korea

폰툰형 초대형 부유체식 부두의 파랑응답해석

이상도[*] · 박성현[**†] · 공길영[***]

* 한국해양대학교 대학원, ** 목포해양대학교, *** 한국해양대학교

Abstract : *In this study, we proposed a pier of pontoon-type, "Very Large Floating Structure" (VLFS), with the length of 500m, breadth of 200 m and height of 2 m in Yeosu domestic port. Since this structure ought to endure wave loads for long periods at sea, it is essential to analyze the wave response characteristics. Direct-method is used to analyze the fluid-structure problem and the coupled motion of equation is used to obtain response results. The structural part is calculated by using finite element method (FEM) and the fluid part is analyzed by using boundary element method (BEM). Dynamic responses caused by the elastic deformation and rigid motion of structure are analyzed by numerical calculation. To investigate response characteristics of the pier in regular waves, several factors such as the wavelength, water depth, wave direction and flexural rigidity of structure are considered. As a result, wave response of pier changed at the point of L/λ 1.5 and represented the torsional phenomenon according to the various incident waves. And the responses showed increasing tendency as the water depths increase at the incident point in case of L/λ=8.0 and peak point of vertical displacement amplitude moved from side to side as the flexural rigidity of structure changes.*

Key Words : *Pontoon-type VLFS, Wave response characteristics, Vertical displacement amplitude, Elastic deformation, Incident wave*

요   약 : 본 연구에서는 국내 여수항만에 길이 500미터, 폭 200미터, 두께 2미터인 폰툰형 VLFS타입의 해상부두를 제안하였다. 이 구조물은 해상에서 오랫동안 파랑하중을 견뎌야하므로 파랑응답해석이 필수적이다. 유체-구조부 해석에는 직접법을 사용하였고, 연성운동방정식을 수치해석하여 응답 결과를 구하였다. 구조부는 유한요소법을 이용하여 계산하였으며, 유체부는 경계요소법을 사용하여 분석하였다. 탄성변형과 강체운동으로 인한 동적응답을 수치적으로 분석하였으며, 파장, 수심, 파향, 구조물의 강성 요소를 고려하여 규칙파에 대한 응답을 해석하였다. 연구의 결과, L/λ 1.5를 기준으로 응답이 변화하였고, 입사파의 방향에 따라 비틀림 현상이 나타났다. L/λ=8.0의 경우 수심이 증가할수록 입사측에서의 응답이 증가하는 경향이 나타났고, 강성의 변화에 따라 수직변위진폭의 피크점이 좌우로 이동하였다.

핵심용어 : 폰툰형 초대형부유체식구조물, 파랑응답특성, 수직변위진폭, 탄성변형, 입사파

1. Introduction

Many countries have been faced with the land scarcity in the process of pier extension and Very Large Floating Structure (VLFS) has been utilized as one of the effective substitute instead of reclamation of sea spaces. As a pier of VLFS is exposed to external wave forces for long periods at sea, it is essential to analyze the response characteristics according to the wave loads. Dynamic response of VLFS due to the wave loads gives rise to the change of pressure of fluid and motion of structure. Such motion of structure comprising elastic deformation means hydroelasticity (Wang et al., 2008).

In order to solve the hydroelastic problem, many researchers use analytical/semi-analytical approach and numerical approach. Voluminous papers related to the hydroelastic response of VLFS have been studied by authors at home and abroad. To analyze the problem of structure part and fluid part, modal method and direct method are commonly used in the frequency domain (Watanabe et al., 2004). We et al. (1995) treated linear two-dimensional problem and extended the eigenfunction expansion-matching method using the modal expansions to analyze the wave-induced responses of VLFS. Takagi et al. (2000) proposed an anti-motion device for VLFS and studied theoretically and experimentally using the eigenfunction expansion method. Kim and Ertkin (1998) also introduced this method for predicting linear hydroelastic behavior a shallow-draft VLFS. Hong et al. (2003) extended Kim and Ertkin (1998)'s eigenfunction expansion method to three dimensions considering the effect of non-zero draft. Because of simplicity and numerical efficiency, Hamamoto and Fujita (2002) used the wet-mode approach to study hydroelastic response of VLFS with arbitrary shape.

In the direct mode, the response of structure is not represented through a superposition of the global modal responses and is determined by directly solving the equation of motion (Watanabe et al., 2004; Wang et al., 2008). This method uses full modes of structure and has a high accuracy for complicated distribution of stiffness (Kim et al., 2006). Yago et al. (1996) modified a direct method using pressure distribution method and compared with the experiment results of a zero-draft VLFS. Yasuzawa et al. (1997) developed a numerical code for dynamic response of mat-type VLFS in regular waves using the direct method. Similar code was applied to container yard and marine pier of VLFS (Park et al., 2003; Lee, 2011).

In this paper, we suggest a pontoon-type pier of VLFS with the length of 500m, breadth of 200m and height of 2m in Yeosu new port. In order to give foundational results for establishing the criteria of VLFS pier, several factors such as the wavelength, water depth, wave direction and flexural rigidity of structure are considered. For the purpose of high accuracy than efficiency, direct method is used to analyze the fluid-structure problem. Dynamic responses caused by the elastic deformation and rigid motion of the pier are analyzed by using numerical calculation. Fluid part is analyzed by using boundary element method (BEM) and structural part is calculated by using finite element method (FEM).

2. Background Theory

Analysis theory is based on the potential theory widely used in terms of the wave loads and estimation of responses. The fluid is assumed inviscid, incompressible and irrotational. Under this assumption, fluid velocity is obtained by derivative of spatial coordinates of velocity potential. Governing equation is the continuity equation and is written by Laplace equation of velocity potentials.

As shown in Fig. 1, we analyze the response characteristics of a floating pier in regular waves, which installed in infinite widespread sea with constant water depth. We formulate respectively the fluid part and structural part, and induce the coupled motion of equation. Analysis should be done under the following assumption (Park et al., 2003; Yasuzawa et al., 1997).

1) The fluid is inviscid, incompressible and the motion of fluid is irrotational and velocity potential is defined.
2) Draft is floating structure can be ignored.
3) Sea bottom is assumed to be flat and sea domain is infinitely extended.
4) Motion of fluid is governed by the linear vibration theory and with regard to deformation, only deflection is considered.
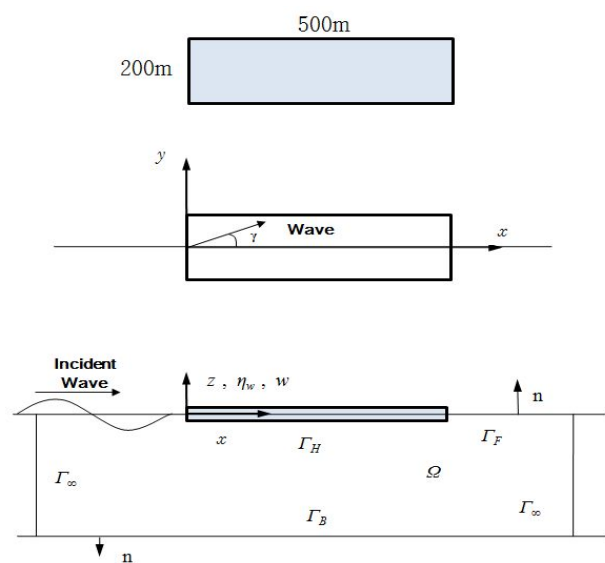5) Damping effect of floating structure can be ignored.

Fig. 1. Model and coordinates of a VLFS for numerical analysis.

2.1 Analysis of fluid part

1) diffraction problem

Fluid part around VLFS is formulated using boundary element method (BEM) and fluid motion is represented using velocity potential. In the analysis model, components of fluid force are potentials by incident wave, diffraction wave and radiation wave. Total potential can be written :

$$\Phi(x,y,z,t) = Re\left[\phi(x,y,z)e^{-i\omega t}\right]$$
$$\phi = \phi_i + \phi_d + \phi_r \tag{1}$$

where ω is the circular frequency of harmonic motion and ϕ_i, ϕ_d, ϕ_r are the incident, diffraction, radiation potentials, respectively. When the structure have no motion and deformation, we seek ϕ_d by diffraction wave. We assume the structure have no motion and deformation as a rigid body, pure boundary value problems of fluid field. As shown in Fig. 1, the boundary value problems can be represented :

$$\nabla^2\phi_d = 0 \qquad\qquad \text{in} \quad \Omega \tag{2}$$

$$\frac{\partial\phi_d}{\partial z} = 0 \qquad\qquad \text{on} \quad \Gamma_B \quad (z = -h) \tag{3}$$

$$\frac{\partial\phi_d}{\partial n} + \frac{\partial\phi_i}{\partial n} = 0 \qquad\qquad \text{on} \quad \Gamma_H \tag{4}$$

$$\frac{\partial\phi_d}{\partial n} - \nu\phi_d = 0 \qquad\qquad \text{on} \quad \Gamma_F \quad (z = 0) \tag{5}$$

$$\lim_{r\to\infty}\sqrt{r}\left(\frac{\partial\phi_d}{\partial n} - i\nu\phi_d\right) = 0 \quad \text{on} \quad \Gamma_\infty \tag{6}$$

$$\nu \equiv \frac{\omega^2}{g} = k\tanh(kh)$$

where n is the outward-directed normal to the fluid domain, g is the acceleration of gravity, k is the wave number and h is the water depth, $\Gamma_B, \Gamma_H, \Gamma_F, \Gamma_\infty$ are boundaries of bottom, body surface, free surface and far-field, respectively.

Laplace equation (2) is governed equation in fluid domain Ω. Boundary condition (3) is represent in constant water depth h The equation (4) is the surface boundary condition in undersurface of structure, equation (5) is the linearized free surface condition, and equation (6) is the radiation condition indicating behavior in the far-field.

2) radiation problem

We regard structure as an elastic body and seek velocity potential ϕ_r generated by motion and deformation of structure. Boundary value problems can be made :

$$\nabla^2\phi_r = 0 \qquad\qquad \text{in} \quad \Omega \tag{7}$$

$$\frac{\partial\phi_r}{\partial z} = 0 \quad \Gamma_B \qquad\qquad \text{on} \quad \Gamma_B \quad (z = -h) \tag{8}$$

$$\frac{\partial\phi_r}{\partial n} = V_n \text{ (n direction velocity)} \text{ on} \quad \Gamma_H \tag{9}$$

$$\frac{\partial\phi_r}{\partial n} - \nu\phi_r = 0 \qquad\qquad \text{on} \quad \Gamma_F \quad (z = 0) \tag{10}$$

$$\lim_{r\to\infty}\sqrt{r}\left(\frac{\partial\phi_r}{\partial n} - i\nu\phi_r\right) = 0 \qquad \text{on} \quad \Gamma_\infty \tag{11}$$

Above problems are same as the diffraction problems, excluding equation (9). Velocity potential ϕ_r can be obtained using boundary element method and integral equation.

3) boundary integral equation

Diffraction problem and radiation problem can be formulated by finite element method using Green function :

$$\int_\Omega \left(G\nabla^2\phi_d - \phi_d\nabla^2 G\right)d\Omega = \int_\Gamma \left(G\frac{\partial\phi_d}{\partial n} - \phi_d\frac{\partial G}{\partial n}\right)d\Gamma \tag{12}$$

Applying the boundary conditions of (2)～(11) in the equation (12), boundary integral equation can be derived :

$$2\pi\phi_d(y) = \int_{\Gamma_H}\left\{G(x,y)\frac{\partial\phi_d}{\partial n}(x) - \phi_d(x)\frac{\partial G}{\partial n}(x,y)\right\}d\Gamma(x) \tag{13}$$
$$x,y \in \Gamma_H$$

$$2\pi\phi_r(y) = \int_{\Gamma_H}\left\{G(x,y)\frac{\partial\phi_r}{\partial n}(x) - \phi_r(x)\frac{\partial G}{\partial n}(x,y)\right\}d\Gamma(x) \tag{14}$$
$$x,y \in \Gamma_H$$

4) Formulation by boundary element method

After dividing integral boundary aspect of (13) and (14) into boundary element, equation is formulated :

$$2\pi\phi(y) = \sum_{j=1}^M \int_{\Gamma_j}\left\{G(x,y)\frac{\partial\phi}{\partial n}(x) - \phi(x)\frac{\partial G}{\partial n}(x,y)\right\}d\Gamma_j(x) \tag{15}$$

where M is the total number of boundary elements. Coordinates of elements and ϕ, $\dfrac{\partial \phi}{\partial n}$ are expressed using linear combination as follows :

$$x(\xi_1, \xi_2) = \sum_{k=1}^{4} N_k(\xi_1, \xi_2) x_k \cdot x_k \qquad (16)$$

$$\phi(\xi_1, \xi_2) = \sum_{k=1}^{4} N_k(\xi_1, \xi_2) \cdot \phi_k \qquad (17)$$

$$\frac{\partial \phi}{\partial n}(\xi_1, \xi_2) = \sum_{k=1}^{4} N_k(\xi_1, \xi_2) \cdot \frac{\partial \phi_k}{\partial n} \qquad (18)$$

where $N_k(\xi_1, \xi_2)$ is shape function. Substituting these into (15) gives

$$2\pi\phi(y_i) = \sum_{j=1}^{M} (\sum_{k=1}^{4} g_{jk} \cdot \frac{\partial \phi_{jk}}{\partial n}) - \sum_{j=1}^{M} (\sum_{k=1}^{4} h_{jk} \cdot \phi_{jk}) \qquad (19)$$

$$g_{jk} = \int_{\Gamma_j} G \cdot N_k(\xi_1, \xi_2) d\Gamma_j$$

$$h_{jk} = \int_{\Gamma_j} \frac{\partial G}{\partial n} \cdot N_k(\xi_1, \xi_2) d\Gamma_j$$

where N is the total nodal point ($i = 1 \sim N$) and ϕ_{jk} is the jth element and kth nodal velocity potential. Arranging these equation concerning corresponding relation of nodal point, matrix equation is derived :

$$[H]\phi = [G] \frac{\partial \phi}{\partial n}, \ [H] = 2\pi[I] + [G] \qquad (20)$$

Substituting each potentials into (20) gives

$$[H]\phi_d = [G] \frac{\partial \phi_d}{\partial n}, \ [H]\phi_r = [G] \frac{\partial \phi_r}{\partial n} \qquad (21)$$

Equation (21) is the final equation of motion in the fluid part.

2.2 Analysis of structural part

Structural part of VLFS is formulated using finite element method. The equation of motion is induced from the principle of virtual work. We regard finite elements as the rectangle plate elements generating bending deformation. Bending displacement of structure can be made :

$$V = N_w \{v\}_e, \quad \{v\}_e = [w_1 \ \theta_{x1} \ \theta_{y1} \ \dots \ w_4 \ \theta_{x4} \ \theta_{y4}]^T \qquad (22)$$

where N_w is shape function and $\{v\}_e$ is the nodal point displacement vector. Because this finite element method is used bending vibration of general plate, we omit detailed theorem (Petyt, 2010).

When the finite element method is applied to the plate generating bending vibration and the equation of motion is induced by principle of virtual work, following equation can be obtained :

$$[K]v + [M]\ddot{v} = \{f\} \qquad (23)$$

where $[K]$ is the stiffness matrix of structure, $[M]$ is the mass matrix of structure, v is the displacement vector and $\{f\}$ is the external force vector.

2.3 Coupled motion equation of fluid and structural part

Coupled motion equation of vibration be induced by connecting the equation of fluid and structural part. Fluctuation pressure $\triangle P$ can be obtained by Bernoulli's theorem :

$$\triangle P = -i\rho_f \omega(\phi_i + \phi_d + \phi_r) - \rho_f g w \qquad (24)$$

where ρ_f is the density of fluid. Total matrix equation can be written :

$$\left[(K + K_w) - \omega^2 M\right]v - i\rho_f \omega C_p \phi_r = i\rho_f \omega C_p(\phi_i + \phi_d) \qquad (25)$$

Collecting equations (21) and (25), simultaneous equation is finally obtained :

$$\begin{bmatrix} (K + K_w) - \omega^2 M & -i\rho_f \omega C_P \\ i\omega GA & H \end{bmatrix} = \begin{pmatrix} v \\ \phi_r \end{pmatrix} = \begin{pmatrix} i\rho_f \omega C_P(\phi_i + \phi_d) \\ 0 \end{pmatrix} \qquad (26)$$

Equation (26) is the final coupled equation of motion in the fluid part and structural part. By solving this equation, nodal displacement vector and nodal velocity potential can be obtained (Park et al., 2004; Petyt, 2010).

3. Numerical analysis of wave responses

Pontoon-type VFLS typically has large horizontal dimensions whereas the height is several meters. Fig. 2 shows the concept of a pontoon-type pier of VLFS with breakwater. In order to use as

marine pier having a capacity for two cargo ships and small yachts, we suggest the VLFS with the length of 500m, breadth of 200m, and height of 2m in Yeosu new port.

We analyzed the wave responses of model A in Table 1. To investigate the response characteristics, this study examined the several factors such as the wavelength, water depth, wave direction and flexural rigidity of structure. We divided the model with 126 nodes and 100 elements. Wave response program is developed and improved by two researchers (Park and Park, 2000).
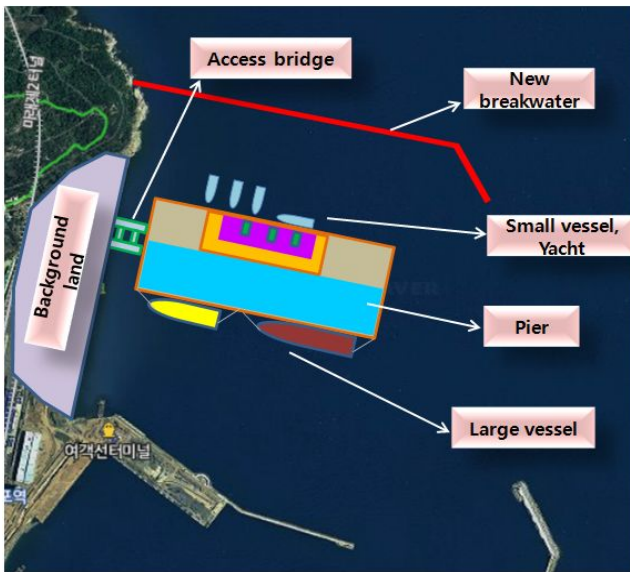
Fig. 2. Concept of a pontoon-type pier of VLFS.

Table 1. Principal particulars of the model for calculation

Dimension	Model A
Length (L)	500 (m)
Breadth (B)	200 (m)
Water depth (h)	10 (m)
Flexural rigidity (D)	4.870E+10 (N/m^2)
Density of sea water (ρ_f)	1.025E +03 (kg/m^3)
Gravity acceleration (g)	9.81 (m/s^2)
Poission's ratio (ν)	0.3
height of plate (t)	2 (m)
Density of plate (ρ_b)	2.563E + 02 (kg/m^3)

3.1 Response characteristics according to the wavelength

We examined the effect of incident waves by changing the ratio of structure length and the wavelength. Fig. 3 shows the corelation between the response amplitude and 3 representative points on the

centerline of structure (incident point, middle point, penetration point). The abscissa L/λ on Fig. 3 indicates the ratio of structure length and the wavelength, and the ordinate $|w|/(H/2)$ represents the ratio of vertical displacement amplitude and wave amplitude. Bending amplitude $|w|$ for L/λ have been divided by the half wavelength. Non-dimensional distribution for the direction of structure length is represented on Fig. 3. The response changed at the point of L/λ=1.5. Due to the large incident wave force, the left side of L/λ=1.5, responses show large amplitude like sea wave. On the contrary, the right side of L/λ=1.5, the penetration side of structure indicates the decreasing curve and elastic responses.
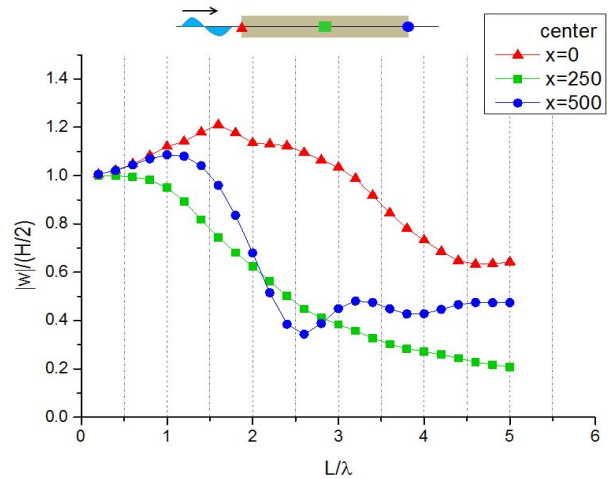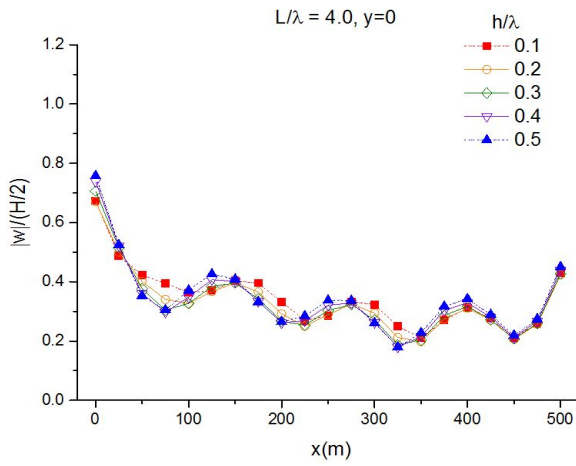

Fig. 3. Wave response characteristics of vertical displacement amplitude depending on L/λ.

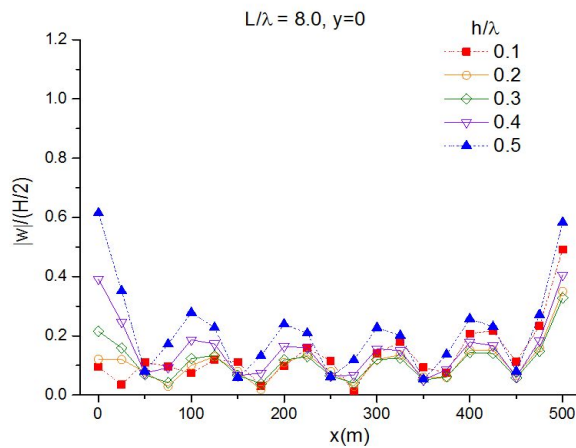### 3.2 Response characteristics according to the water depth

In this part, we examined the responses according to the ratio of water depth and the wavelength. Shin et al. (2000) studied that the vertical displacement amplitude in the depth of 8m is smaller than the depth of 58.5m. Kyoung et al. (2005) investigated that the hydroelastic responses are influenced by the sea bottom topographies rather than the change of sea depths.

We calculated by changing h/λ and compared the results as shown in Fig. 4. Wave responses are not considerably influenced by the change of depths in case of L/λ=4.0 whereas the responses show increasing tendency as the depths increase at the incident point in case of L/λ=8.0. The results feature the elastic responses due to the influence of seabed and slight variation of vibration mode due to the wavelength.

(a)

(b)

Fig. 4. Comparison of vertical displacement amplitude depending on the h/λ : (a) L/λ=4.0, y=0 and (b) L/λ=8.0, y=0.
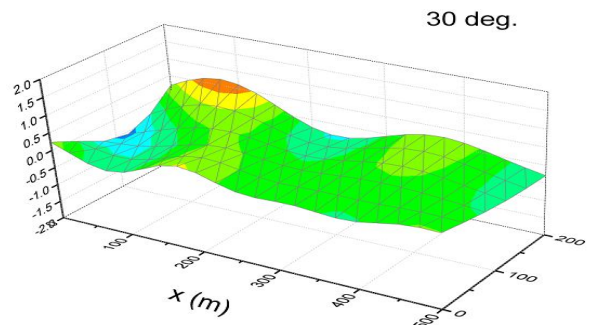
3.3 Response characteristics according to the direction of incident waves

This part deals with the response characteristics according to various incident wave direction. We analyzed the responses by changing the incident wave angles like 0 degree (a), 30 degree (b), 50 degree (c), 80 degree (d) in case of L/λ=4.0 waves.
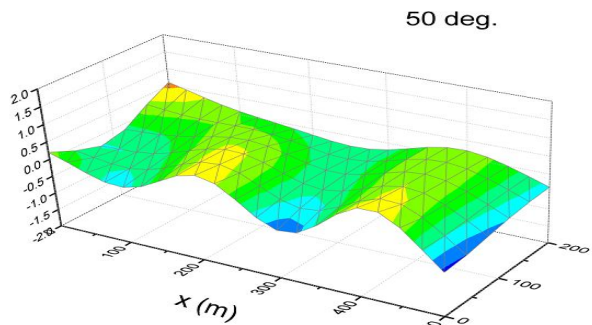
Fig. 5 represents the torsional phenomenon according to the incident waves. The maximum point of displacement varies with the wave directions. It was found that the maximum point of response does not correspond with the incident wave angles.
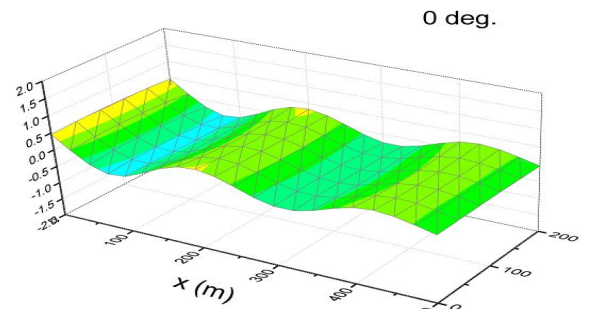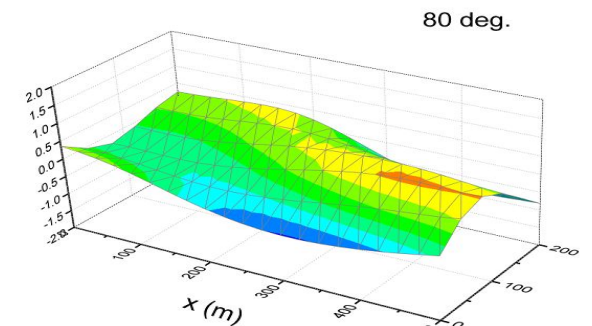

(a)

(b)

(c)

(d)

Fig. 5. Response results of real displacement according to incident waves for L/λ=4.0 : (a) incident angle 0 deg., (b) incident angle 30 deg., (c) incident angle 50 deg., and (d) incident angle 80 deg.

3.4 Response characteristics according to the Flexural rigidity of structure

This part analyzed the response characteristics by changing flexural rigidity of structure. Responses of model B are shown on Fig. 6 and D is the flexural rigidity of structure. The flexural rigidity (D) of (a) is 100 times larger than model A, (b) is 10 times smaller than model A, and (c) is 100 times smaller than model A. When the flexural rigidity of structure increases, peak point of L/λ moves left side and responses decrease at the large L/λ ratio. On the contrary, peak point of L/λ moves right side in case the flexural rigidity of structure decreases. Peak point of vertical displacement amplitude moves from side to side according to flexural rigidity of structure. When the flexural rigidity of structure increases, elastic response is dominant. On the contrary, lower flexural rigidity of structure shows a form of riding waves despite decrease of the wavelength.
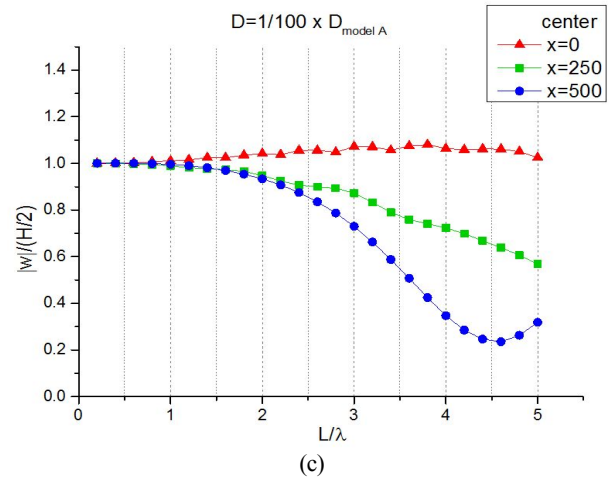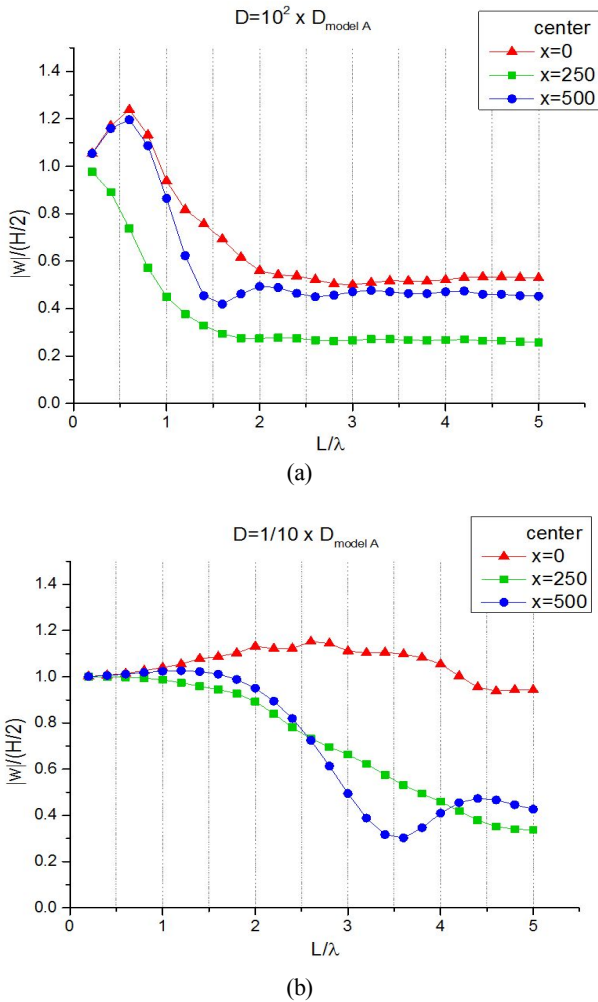

(a)

(b)

(c)

Fig. 6. Response results according to flexural rigidity of structure : (a) $D=10^2 \times D_{modelA}$, (b) $D=1/10 \times D_{modelA}$, and (c) $D=1/100 \times D_{modelA}$.

4. Conclusion

We analyzed the wave response characteristics of a suggested pontoon-type pier of VLFS in Yesou new port using the direct method and obtained following results according to the several factors such as the wavelength, water depth, wave direction and flexural rigidity of structure.

(1) Wave response changed at the point of $L/\lambda=1.5$. Responses show large amplitude like sea wave on the left side of $L/\lambda=1.5$ and the penetration side of structure indicates the decreasing curve and elastic responses.

(2) The responses show increasing tendency as the depths increase at the incident point in case of $L/\lambda=8.0$. The results feature the elastic responses due to the influence of seabed and slight variation of vibration mode due to the wavelength.

(3) Torsional phenomenon are shown according to the various incident waves. The maximum point of displacement varies with the wave directions.

(4) Peak point of vertical displacement amplitude moves from side to side as the flexural rigidity of structure changes. Elastic response is dominant in case flexural rigidity increases whereas lower flexural rigidity of structure shows a form of riding waves despite decrease of the wavelength.

The effect of changing depths is debatable point because this study is investigated in the range of comparatively shallow depths considering local area of Yeosu new port. Also, future study is needed about overall safety evaluation of the pier of VLFS for actuality to the domestic port.

References

[1] Hamamoto, T. and K. Fujita(2002), Wet-Mode Superposition for Evaluating the Hydroelastic Response of Floating Structures with Arbitrary Shape, Proceedings of the 12th International Offshore and Polar Engineering Conference, Kitakyushu, Japan, pp. 121-128.

[2] Hong, S. Y., J. W. Kim, R. C. Ertekin and Y. S. Shin(2003), An Eigenfunction Expansion Method for Hydroelastic Analysis of a Floating Runway, Proceedings of the 13th International Offshore and Polar Engineering Conference, Honolulu, Hawaii, pp. 121-128.

[3] Kim, B. W., S. Y. Hong, J. H. Kyoung and S. K. Cho(2006), Investigation on Wave Reduction Performance of Floating Hinge-Linked Breakwater, Journal of Ocean Science and Technology, Vol. 3. No. 1, pp. 13-22.

[4] Kim, J. W. and R. C. Ertekin(1998), An Eigenfunction Expansion Method for Predicting Hydroelastic Behavior of a Shallow-draft VLFS, Proceedings of the Second International Conference on Hydroelasticity in Marine Technology, Fukuoka, Japan, pp. 47-59.

[5] Kyoung, J. H., B. W. Kim, S. K. Cho and S. Y. Hong(2005), Numerical Study on the Hydroelatic Response of the Very Large Floating Structure Considering Sea-Bottom Topography, Journal of the Society of Naval Architects of Korea, Vol. 42. No. 4, pp. 357-367.

[6] Lee, S. D.(2011), A Study on the Wave Response for Eco-friendly Marine Wharf of the Very Large Floating Structure, Master Thesis, Mokpo National Maritime University.

[7] Park, S. H. and S. C. Park(2000), A Study on the Reduction Analysis of the Response of the Mega-Float Offshore Structure in Regular Wave, Journal of Korean Navigation and Port Research, Vol. 24, No. 1, pp. 85-95.

[8] Park, S. H., S. C. Park and J. Y. Koo(2003), A Study on the Container Yard of Mega-Float Offshore Structure Type, Journal of Korean Navigation and Port Research, Vol. 27, No. 1, pp. 49-54.

[9] Park, S. H., S. C. Park, M. C. Choi and J. Y. Koo(2004), Study on the Optimization of Response in Regular Wave of the Mega-float Offshore Structure, Proceedings of the Spring Meeting, The Korean Society of Marine Environment & Safety, pp. 99-105.

[10] Petyt, M.(2010), Introduction to Finite Element Vibration Analysis, Second Edition, Cambridge University Express, pp. 119-247.

[11] Shin, H. K., H. Y. Lee, H. S. Shin and I. K Park(2000), Analysis Methods of Hydroelastic Responses for a Very Large Floating Structure, The Korean Society of Ocean Engineers, Vol. 14, No. 2, pp. 19-27.

[12] Takagi, K., K. Shimada and T. Ikebuchi(2000), An Anti-motion Device for a Very Large Floating Structure, Marine Structure, Vol. 13, pp. 421-436.

[13] Wang, C. M., E. Watanabe and T. Utsunomiya(2008), Very Large Floating Structure, Taylor & Francis, pp. 35-65.

[14] Watanabe, E., T. Utsunomiya and C. M. Wang(2004), Hydroelastic Analysis of Pontoon-type VLFS: a Literature Survey, Engineering Structure, Vol. 26, pp. 245-256.

[15] We, C., E. Watanabe and T. Utsunomiya(1995), An Eigenfucntion -matching Method for Analyzing the Wave-induced Responses of an Elastic Floating Plate, Applied Ocean Research, Vol. 17, pp. 301-310.

[16] Yago, K., S. Ohmatsu and H. Endo(1996), On the Hydroelastic Response of Box-Shaped Floating Structure with Shallow Draft : Tank Test with Large Scale Model, Journal of the Society of Naval Architects of Japan, No. 180, pp. 341-352.

[17] Yasuzawa, Y., D. Kawano, K. Kagawa and K. Kitabayashi (1997), Numerical Response Analysis of a Large Mat-type Floating Structure in Regular Waves, Journal of the Society of Naval Architects of Japan, No. 181, pp. 111-122.